Broadband Low-Loss On-Body UHF to Millimeter-Wave Surface Wave Links using Flexible Textile Single Wire Transmission Lines

Mahmoud Wagih, *Member, IEEE*

***Abstract*—On-body transmission represents a challenge due to human body shadowing. This paper proposes a Sommerfeld-Goubau single-wire transmission line (SWTL) implemented using electronic textiles for low-loss on-body links up to millimeter-wave frequencies, overcoming the spherical spreading loss and on-body absorption. The SWTL is fabricated using a conductive thread suitable for embroidery on textiles. A compact tapered launcher is implemented on a flexible polyimide substrate to excite the surface mode along the SWTL. In space, a 3 m-long line maintains a forward transmission over −10 dB between 1 and 3 GHz. The SWTL link is characterized for different body parts showing under 20 dB insertion loss with a 1 cm air gap. Across the torso, a forward transmission over −20 dB is maintained from 0.5 to 2.5 GHz, which represents at least 20 dB improvement over two antennas, of larger dimensions, over-the-air. Directly on-skin, the SWTL can be used around 1 GHz with an S_{21} over −25 dB, over 50 dB improvement over two on-skin antennas. At 50 GHz, the shielded SWTL exhibits an ultra-low on-body attenuation around 0.11 dB/mm, a four-fold improvement over a microstrip line on the same substrate. It is concluded that SWTLs can enable ultra high-speed future body area networks.**

***Index Terms*—Antennas, Body Area Networks, Coplanar Waveguides, Metamaterials, On-Body Communications, Single Wire Transmission Line, Textile Metamaterials, Textile Transmission Line, Wearables.**

I. Introduction

BODY Area Networks (BANs) have attracted significant research interest for reliably connecting and powering wearable devices [1]–[3], often implemented using flexible and textile-based materials [4]–[7]. Central to pervasive BANs are wearable flexible and textile-based antennas [7], [8]. To realize a wireless link between two wearable devices located on the same user, "on-body" antennas with omnidirectional or end-fire patterns are typically used [9]. However, it is widely known that ultra high frequency (UHF), microwave, and millimeter-wave (mmWave) radiation above few hundred MHz attenuate significantly near the body, which reduces the channel gain between on-body antennas [1], [2], [10]. For example, the losses in the skin layer increase significantly at mmWave frequencies [11]. Moreover, the wireless forward transmission betwen wearable antennas is highly dependent on the body position and activity [12].

On-body wireless communications have two key advantages. First of all, avoiding the need for cumbersome interconnections required to transfer data using on-body interconnects [13]. To explain, transferring digital information with data-rates exceeding a few kilobits per second requires complex e-textile buses [14], which increases the amount of conductive material required to realize a wired network of wearable devices compared to a wireless solution [3]. Therefore, a range of on-body antennas have been developed to maximize the channel gain between wearable devices [15]–[17].

The additional advantage of on-body RF links is enabling high data-rate communication between wearables located on the same body or garment [18]. To explain, low-frequency "wired" serial protocols are limited to data-rates under 20 MBPS, making them unsuitable for applications requiring a large amount of data to be transmitted. A range of low-cost low-power modulators and transceivers have been demonstrated with GBPS data-rates, which could be applied in future BANs. The high data-rate is achieved by operating in the mmWave spectrum such as the 24 GHz [19], and 60 GHz [20], license-free bands. Therefore, high channel gain wireless links [21] and low-loss textile-based waveguides [22] are required to enable high data-rate communication on-body. However, the on-body attenuation cannot be ignored, where low-loss on-body links, especially in the mmWave spectrum, are only achievable using highly directional antennas such as non-textile horns [21]. To reduce the on-body losses, a conductive textile stripline was proposed, reducing the losses between two on-body patch antennas by at least 10 dB [23]. Nevertheless, this approach was limited in bandwidth and only demonstrated at 2.4 GHz. Furthermore, the combined thickness of the stripline and the patch (>7 mm) is unsuitable for "low-profile" e-textile applications [24].

Through-body propagation, human-body communications (HBC), and e-textile low-frequency magneto-inductive waveguides are among the implementations proposed to address the issue of UHF radiation/body interaction. Utilizing body-confined electric or magnetic fields under 100 MHz, low-loss links can be realized between multiple on-body devices for transferring data and power [2], [10], [25]. Nevertheless, the low frequency of operation of such links limits the data-rates which can be achieved using such links.

More recently, a textile-based metamaterial, based on spoof-surface plasmons (SSPs), was used to realize low-loss on-

This work was supported by the UK Engineering and Physical Sciences Research Council (EPSRC) under Grant EP/P010164/1 and jointly by the UK Royal Academy of Engineering and the Office of the Chief Science Adviser for National Security under the UK Intelligence Community Research Fellowship programme.

The authors is with the School of Electronics and Computer science, University of Southampton, Southampton, SO17 1BJ, U.K. (email: mahm1g15@ecs.soton.ac.uk)

Digital Object Identifier: .

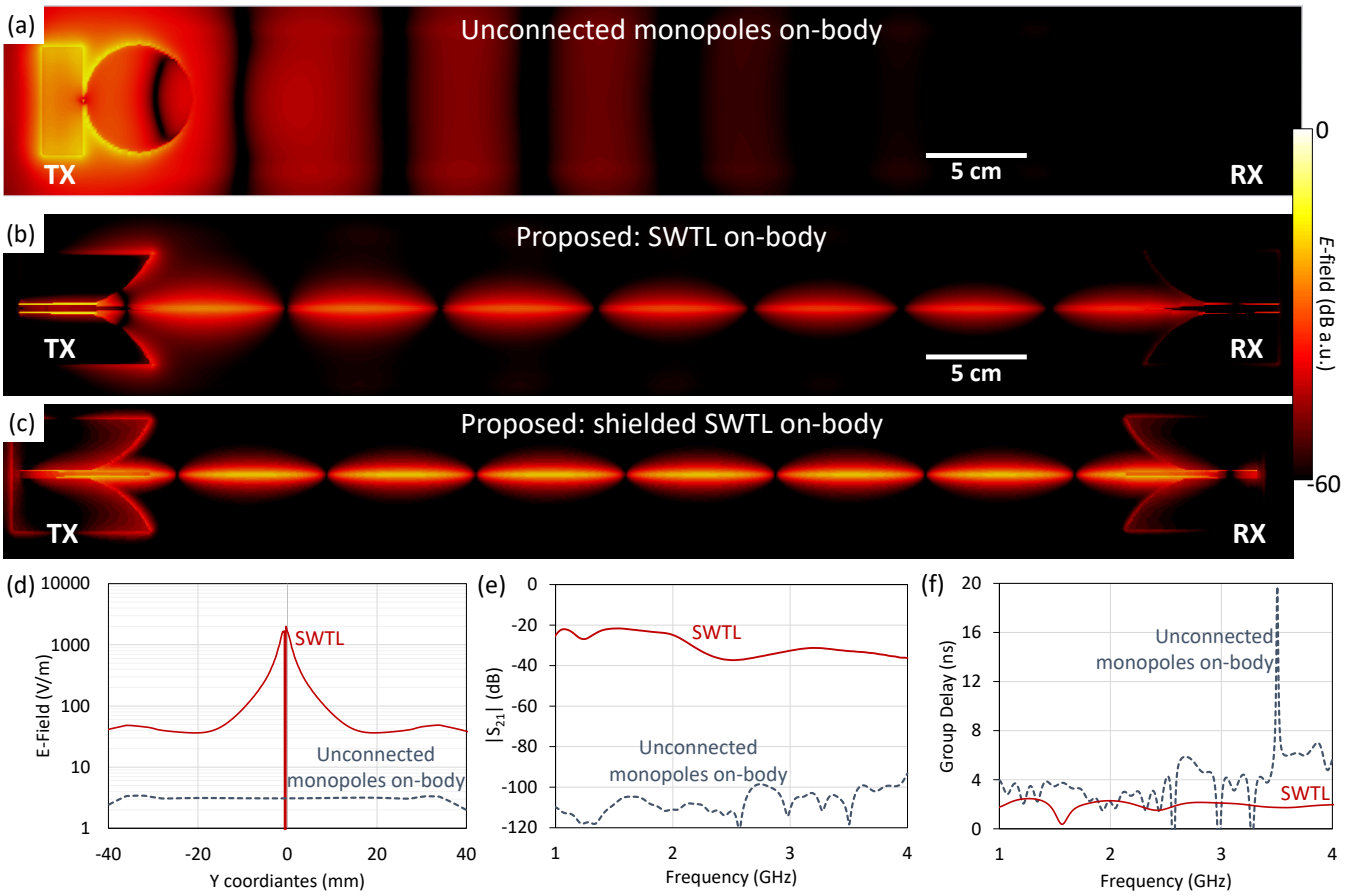

Fig. 1. Simulated performance of an on-body SWTL compared to unconnected omnidirectional monopoles for a 45 cm link at 2 GHz: (a) E-field plot of unconnected on-body monopoles (benchmarking reference); (b) E-field plot of the proposed on-body SWTL; (c) E-field plot of the proposed on-body SWTL backed by a shielding conductive plane; (d) 1D E-field cross-section at half-way through the link, i.e., at 22 cm from the transmitter; (e) the forward transmission betwen the two on-body ports; (f) the group delay of the OTA link and the SWTL.

body interconnects at 2.4 GHz [1], as well as omnidirectional off-body radiation patterns overcoming body shadowing [26]. The aforementioned metamaterial leverages surface-wave propagation near the body, where the surface-wave SSP is matched to a standard microstrip line, which can interface with off-body microstrip antennas and wearable circuitry. Owing to its shielding from the body, the SSP does not incur additional losses to the body. Surface-wave modes have also been investigated for long-range RFID using a Single-Wire Transmission Line (SWTL), excited using a 3D horn-like launcher [27]. To date, SWTLs have not been applied to wearable applications, and the interaction of surface-waves with the human body has not been investigated or compared to unconnected propagation between on-body antennas. Furthermore, despite Goubau SWTLs being demonstrated up to sub-THz bands using nano-fabricated lines [28], there has been no report of a wearable SWTL, or any wearable surface wave transmission line operating in the mmWave spectrum.

In this paper, the use of textile SWTLs as a mean of low-loss broadband on-body transmission up to 50 GHz is proposed, representing the first use of a broadband SWTL on-body. Compared to radiative transmission, it is shown that the on-body SWTL can improve the forward transmission by at least 20 dB. A wearable low-loss mmWave on-body link supported by a shielded e-textile SWTL is then proposed for the first time, demonstrating a four-fold improvement over a state-of-the-art textile-based microstrip line. In Section II, the design of the launcher and SWTL simulated results are presented, with the experimental characterization of the SWTL on different body parts and in space presented in Section III.

II. SWTL and Launcher Design and Simulation

A Goubau SWTL supports conformal surface wave propagation, enabling a lower loss compared to conventional TEM transmission lines [27], as well as over-the-air (OTA) wireless propagation [1]. Nevertheless, there has been no implementation of an on-body unshielded SWTL, where it is expected that the SWTL will experience higher losses due to absorption by human tissue.

To understand the body/SWTL interaction, a 45 cm-long SWTL has been simulated in CST Microwave Studio and compared to two unconnected broadband monopoles, based on broadband disc antennas [24], [29]. The link is located at 5 mm from a layered tissue (3 mm-thick skin, 2 mm-thick fat, and 8 mm muscle) model. In addition to the SWTL, a conductor-backed SWTL, with a 1 mm separation, has also been simulated to isolate the SWTL from the body-induced losses. The response of both the OTA link and the two

Goubau SWTLs is shown in Fig. 1. As expected, the OTA monopoles, radiating omnidirectionally, result in a very low E-field density at the receiver. This is attributed to the attenuation by the human tissue in close proximity, as well as the low confinement of the fields, as visualized in Fig. 1(a)–(c).

Observing Fig. 1(a), the radiative link between two omnidirectional monopoles results in a very low E-field density at the receiver (RX) under -60 dB normalized to the maximum E-field. The path loss also increases due to the attenuation by the human tissue underneath the antenna. On the other hand, Fig. 1(b) shows a significantly higher E-field density at RX when using an SWTL with tapered "Vivaldi" launchers. The improved forward transmission is attributed to the higher confinement of the E-fields around the surface of the dielectric-coated Litz wire. The link's efficiency is further improved by shielding the SWTL using the unconnected (e-textile) metal plane. Observing Fig. 1(c), it can be seen that a higher E-field density is maintained along the line as well as at RX; the tissue losses have been nearly eliminated by the existence of a conductive plane.

A 1-dimension E-field cross-section halfway through the link, i.e. at 22 cm from the transmitter, is shown in Fig. 1(d). It can be seen that E-field around the SWTL is orders of magnitude higher than that in the monopole's far-field. The observed drop in the E-field in Fig. 1(d) at 0 mm is the location of the SWTL, modeled as a 0.3 mm-thick wire. The higher and more confined E-field propagation results in over 60 dB simulated forward transmission improvement in the 1–4 GHz spectrum, as shown in Fig. 1(d). Moreover, the confined TM surface wave mode exhibits a more uniform phase response, which manifests through the more stable group delay, visible in Fig. 1(f).

Based on the simulated response, an unshielded SWTL enables low-loss on-body links in the UHF spectrum. A launcher was then designed based on a coplanar waveguide (CPW) tapered "Vivaldi" structure [28], to excite the on-body SWTL. The launcher is designed to interface the SWTL to other 50 Ω transmission lines [30]. The mode conversion takes place at the launcher between the 50 Ω-matched TEM or Quasi-TEM transmission line, and the TM surface wave mode. A Vivaldi-inspired CPW launcher has previously been developed for exciting SWTLs [31]. Nevertheless, it was based on a 3-dimensional structure and utilizes a large metal plate as a reflector, making it unsuitable for wearable applications. On the other hand, the proposed design is planar, single-sided, and can be implemented on thin and flexible substrates. Fig. 2(a) shows the dimensions of the SWTL launcher and the SWTL in Fig. 2(b). The dimensions (w_f and g) of the CPW feed were chosen to maintain a Z_0=50 Ω.

To demonstrate the safety of the SWTL for use on-body, the power losses along the SWTL have been simulated at different frequencies between 1 and 4 GHz, to evaluate the Specific Absoprtion Rate (SAR). Two simplified tissue models were designed in CST Microwave Studio, where utilizing a high-resolution full-body model such as CST's Hugo will result in a very fine mesh leading to a very intensive computation. Fig. 3 shows the simulated SAR along the unshielded SWTL.

The power of the excitation signal at which the SAR has been calculated was set to approximately the maximum power level which results in an SAR under 1.7 W/kg, which complies with the IEEE C95.1 regulations. It can be seen that at lower frequencies, a higher power level (0.5 W) could be carried safely by the SWTL owing to the lower human body absorption. As the frequency increases to 4 GHz, the maximum compliant power level drops to 17 dBm. In most on-body communication applications, the power level transmitted will likely remain under 0 dBm, especially with the high S_{21} offered by the SWTL. Nevertheless, the safe relatively high power handling capability of the unshielded SWTL demonstrates its suitability for on-body RF power transmission as well as feed-lines for high-power transmitters. As for the shielded SWTL, the simulated SAR for a 0.5 W input was under 0.1 W/kg, attributed to the high isolation offered by the conductive plane between the SWTL and the body.

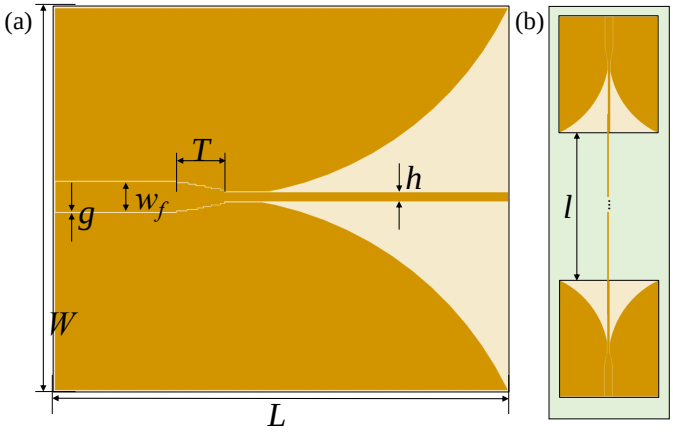

Fig. 2. Layout and dimensions of the proposed SWTL: (a) CPW surface wave launcher; (b) the SWTL with the transmit and receive launchers; dimensions in mm: L=61, W=50.5, t=6.5, w_f=4.5, g=0.15, h=1.2.

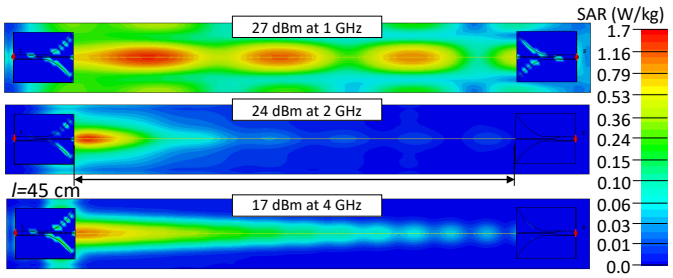

Fig. 3. Simulated SAR across an unshielded textile SWTL with l=45 cm at different frequencies over a uniform multi-layered tissue model; the input power level is the maximum which satisfies the 1.7 W/kg requirement.

III. Results and Discussion

A. Launcher and SWTL Fabrication

To fabricate the proposed SWTL using wearable-friendly materials, two common e-textile fabrication methods are used: flexible circuit photolithography and embroidery. First of all, the launchers in Fig. 2 were fabricated using photolithography on thin and flexible polyimide copper laminates. This approach has been widely used to realize textile-based RF components with low conductive losses and high efficiency up to mmWave

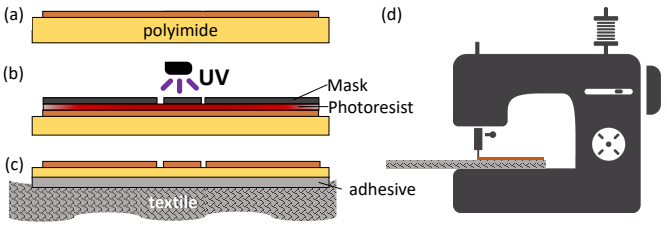

Fig. 4. Fabrication steps of the e-textile SWTL: (a) flexible polyimide (Kapton) copper laminate; (b) photolithography of the launcher's patterns using UV exposure and chemical etching [7]; (c) attachement of the flexible polyimide-based laucnher/circuit onto the textile substrate [6]; (d) over-stitching of the fabric Litz thread onto the same textile substrate [32].

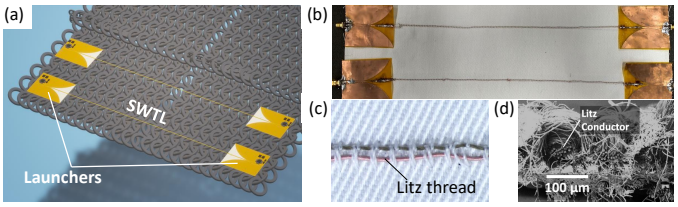

Fig. 5. Two closely-packaged SWTLs on a polyester cotton substrate: (a) 3D mockup showing the possible component placement on the launchers; (b) photograph of the fabricated lines; (c) micrograph showing the over-stitched wire; (d) scanning electron microscope (SEM) cross-section of the Litz wire in-fabric.

bands [7], owing to the high conductivity and low roughness of flexible copper sheets compared to printed or electroplated conductors [6]. The Litz e-textile threads were then over-stitched on the same textile substrate before being soldered directly on the end of the CPW signal traces of the launchers, as shown in Fig. 2(b). The fabrication steps are shown in Fig. 4, with photographs of the fabricated two-line prototype, including the wire's micrographs, visible in Fig. 5.

The polyimide-based launchers can be attached to the textile substrate using an adhesive layer or heat-pressing, using a polyurethane interface [6]. The electric shielding (for the shielded SWTL) is then realized using electroplated conductive fabric (P&P Metweave), previously used to realize high-efficiency antennas [33]. Polyimide copper laminates were chosen for the launchers due to their favorable thermal and mechanical properties, making them suitable for integration with the driving circuitry, as well as for realizing small features of the impedance-controlled transmission line, such as the CPW gaps [34]. Furthermore, a higher mechanical reliability as well as a fully-waterproof structure can be realized to withstand machine washing based on an additional encapsulant layer, such as heat-pressed polyurethane [6], or vacuum-formed polyimide [35].

B. SWTL In-Space and On-Body Transmission Measurements

A two-port Rhode and Schwarz ZVB4 Vector Network Analyzer (VNA) was used to measure the s-parameters of the SWTL. The measurements were performed in space as well as for different on-body positions. The on-body links are shown in Fig. 6. Prior to characterizing the SWTL over the human body, the SWTL and launchers were characterized in space. Three lines of different length l were fabricated and measured experimentally. Fig. 7(a) and (b) show the measured forward transmission and reflection coefficient, respectively, of the unloaded lines. A photograph of the 120 cm-long line measurement setup is shown in Fig. 6(b). As the SWTL was simulated using a simple layered tissue model, the forward transmission properties of the SWTL over different body parts are characterized experimentally. To explain, due to the length of the line and its μm-scale thickness, a very fine mesh will be required to model the on-body conformable line in full-wave simulations. Therefore, the simulated results are only included as indicative "on-body" performance, which does not reflect the variations due to different tissues' dielectric properties, or due to bending around the body.

Observing the measured response in space, it can be seen that the lines maintain an S_{11} under -6 and -10 dB, from 1.6 and 2.4 GHz, respectively, and up to 3 GHz. The S_{21} closely follows the S_{11} response, where the forward transmission improves at the frequencies where reflection minimas are observed, resulting in a small ripple around ± 2 dB. While this response indicates that the impedance matching between the TEM mode, in the coaxial connectors, to the surface-wave mode can be improved, the measured minimum attenuation of α=0.019 dB/mm at 1.6 GHz is in-line with recently reported SWTLs, e.g., [31], which maintain a minimum α=0.023 dB/mm. Furthermore, the observed relatively high S_{11} only represents a design issue for transmitters which cannot withstand a Voltage Standing Wave Ratio (VSWR) over 2.0, such transmitters often utilize high-power and high-gain power amplifiers, not typically found in real-world low-power and low-cost wearable and IoT applications. To explain, most on-body applications are expected to operate around or below 0 dBm, where a range of Internet of Things (IoT) antennas operating at such power levels were designed for an $S_{11} < -6$ dB specification [36].

The SWTL link has been characterized for different on-body positions, shown in Fig. 6(a). A shorter SWTL with l=45 cm was used for the on-body measurements. The first link, L_1, is for the SWTL conforming to the user's chest. In this setup, the launchers are located behind the user's back, with the SWTL wrapping around the user's chest. Therefore, there is no alignment between the "end-fire" launchers, and a conformal surface wave mode is required to maintain a high S_{21} link. Similarly, in link L_2, the SWTL surrounds the user's waist with no direct line-of-sight alignment between the CPW launchers. L_2 represents a potential application where an SWTL could be packaged within a belt, where belts have recently been used as off-body antennas [37]. In link L_3, whose photograph is shown in Fig. 6(c), the SWTL goes from the user's chest to below the waist, along a thin polyester fabric layer. The SWTL is also characterized along the arm in link L_4, whose photograph is shown in Fig. 6(d). Along the arm, the bending effects can be further investigated to validate the conformal propagation along the body. The same SWTL length l of 45 cm was used for all links to observe the human body absorption effects. An air gap not exceeding 1 cm was present between the SWTL and the body in all the test setups.

Fig. 8 shows the measured s-parameters of the SWTL over the different body parts considered, as well as the same 45 cm-

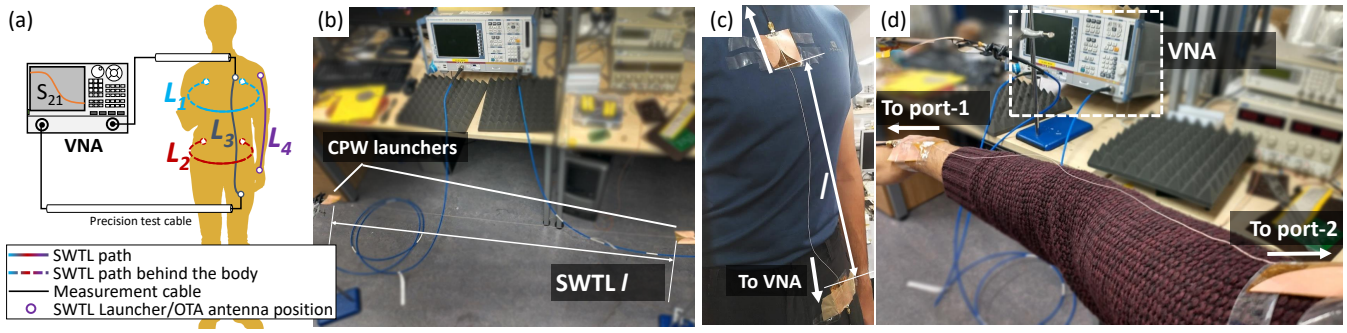

Fig. 6. The on-body measurement setup of the SWTL: (a) positions of the on-body links investigated; (b) photograph the in-space SWTL measurement setup; (c) photograph of link L_4; (d) photograph of link L_3.

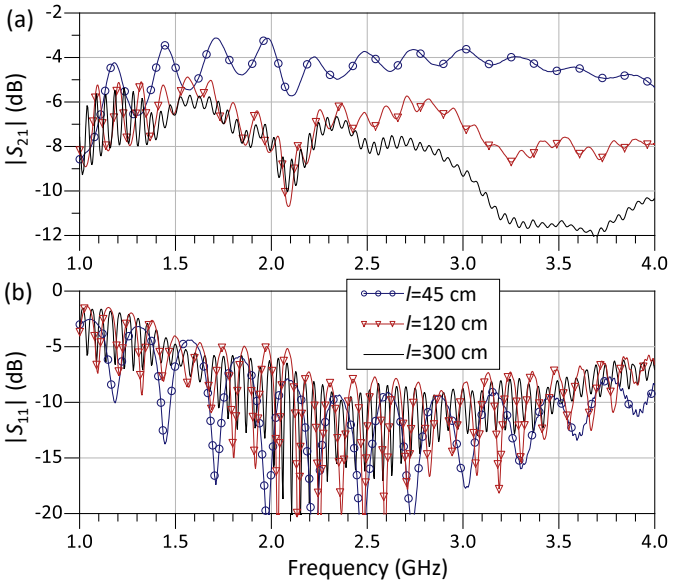

Fig. 7. Measured s-parameters of the SWTL with different lengths in space using the setup in Fig. 6(b): (a) forward transmission; (b) reflection coefficient.

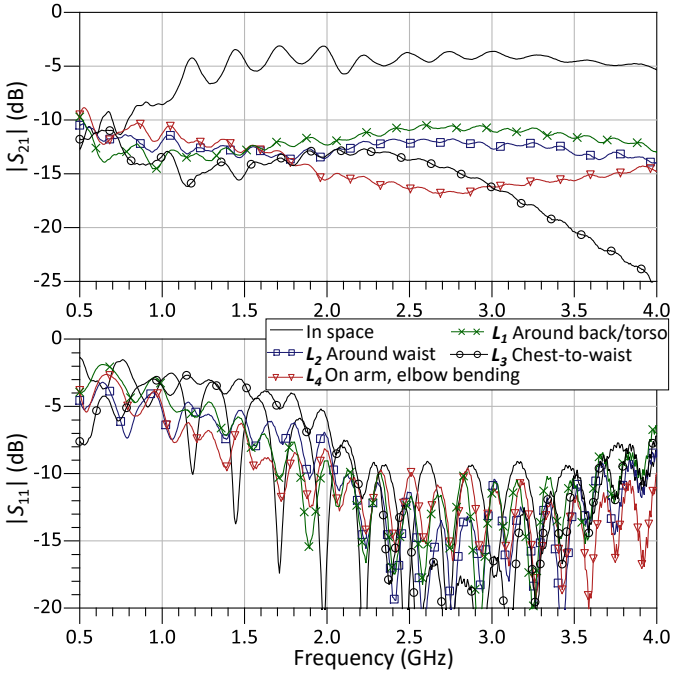

Fig. 8. Measured s-parameters of the SWTL over for the different on-body links, whose test setups are shown in Fig. 6(a).

long SWTL in space. The highest loss is observed when the surface wave propagation encounters a discontinuity, i.e. the on-arm elbow bending case. When the SWTL was wrapped around the user's belt, the increase in the insertion loss over the free-space SWTL is under 7 dB, compared to the free-space SWTL. In addition, over all measured cases, it can be observed that the SWTL maintains a matched 10 dB return loss from 2.2 to 3.7 GHz, a fractional bandwidth over 40%.

C. Comparison with Over-the-Air Links

A key advantage of the on-body SWTL is reducing the transmission losses relative to on-body antennas. For benchmarking, two on-body broadband disc monopoles [29] were used to measure the channel gain on-body in the same test positions. The discs were scaled to cover the UHF spectrum and implemented on a felt substrate, following the design and fabrication process reported in [24]. Moreover, the S_{21} between the CPW launchers without a SWTL has also been measured. Fig. 9 shows the measured S_{21} of the SWTL, the OTA monopoles, and the unconnected launchers. The measurements were performed with a variable air gap measured to be under 5 mm, as well as with the SWTL, antennas, or launchers, pressed against the body with $<$1 mm fabric separation.

Observing Fig. 9, the proposed SWTL improves the link at a modest skin-SWTL air gap around 5 mm by over 20 dB across the full 0.5–4 GHz spectrum. As for the direct body contact case, the measured S_{21} exhibits a uniform decrease with increasing frequency up to 2 GHz, which is linked to the increasing tanδ loss through the tissue with frequency. The simulated S_{21} shown in Fig. 9 exhibits the same trend as the measured results with variations between 5 and 10 dB. The discrepancy observed is attributed to the tissue model being a uniform and homogeneous rectangle, whereas the human body will exhibit different dielectric properties to the simplified layered model. In both the 5 mm-separated and the on-body SWTL, it can be observed that the SWTL exhibits an improved S_{21}, while occupying a smaller physical area, owing to the more compact launcher compared to sub-1 GHz broadband monopoles.

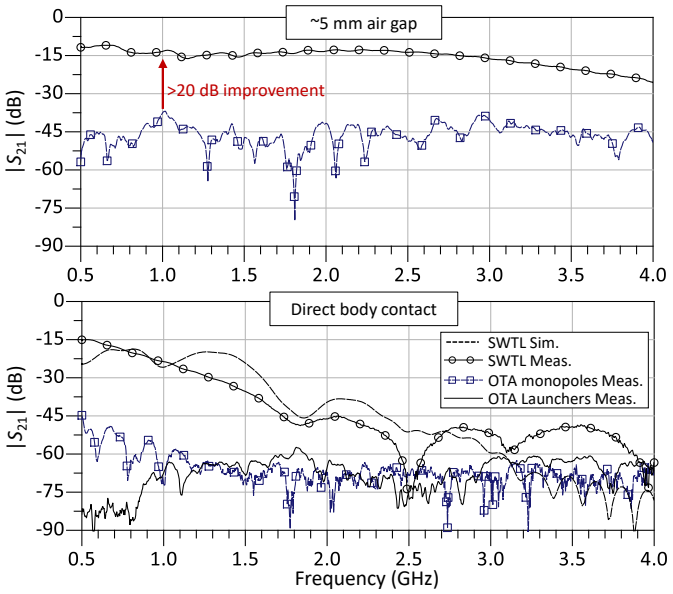

Fig. 9. Comparison of the on-body unshielded SWTL performance relative to unconnected on-body monopoles and launchers: (a) link L_3 from Fig. 6(a) with a 5 mm air gap between the SWTL and the body; (b) link L_2 with the SWTL, launchers, and OTA antennas pressed against the body with no gap.

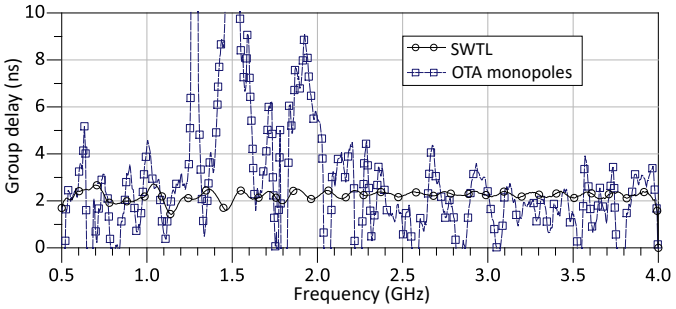

Fig. 10. Measured group delay of the SWTL and the on-body monopoles for a chest-to-waist link, shown in Fig. 6(b).

An additional advantage in broadband signaling, e.g. UWB communications, using the proposed e-textile SWTL is the more stable phase response. The group measured group delay of the SWTL and the OTA monopoles for the chest-to-waist link is shown in Fig. 10. For the SWTL, the maximum group delay ripple is ± 0.64 ns, off the mean group delay of 2.16 ns. On the other hand, the group delay between the on-body unconnected monopoles exhibits a significant ripple in excess of 10 ns. Therefore, UWB communication between on-body devices could be realized using the proposed SWTL, owing to the uniform phase response and the broadband S_{21} improvement over the unconnected OTA antennas.

D. SWTL Continuity and Immunity to Interference

As the SWTL supports a conformable surface-wave TM mode as opposed to a TEM [38], or quasi-TEM mode [6], it is expected to maintain an resilience to small gaps along the line [1]. Such gaps will prevent any DC/low-frequency currents from flowing through the line, as well as act as an open termination resulting in standing waves along a traditional transmission line [26]. To explain, a gap across a planar transmission line will exhibit minimal capacitance, which will not be sufficient to allow UHF signals to propagate through the transmission line [6]. The proposed SWTL was measured before and after cutting to demonstrate its resilience to mechanical damage. The Litz wire, attached to the textile substrate using the over-stitched thread was cut horizontally at different positions. The line's S_{21} was measured after each cut; the cuts were separated by approximately 10 cm. Fig. 11 shows the measured S_{21} of the SWTL before and after cutting.

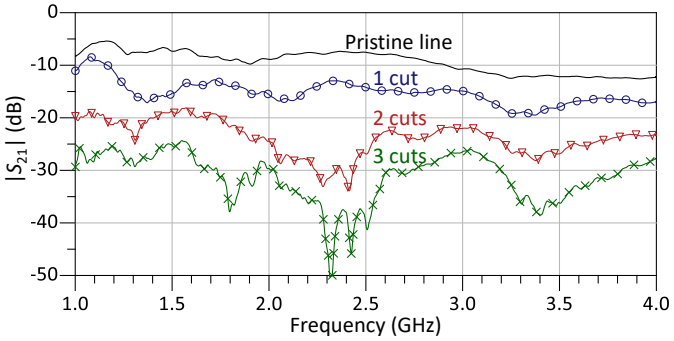

Fig. 11. Measured forward transmission of the 45 cm-long SWTL for a different number of 10 cm-spaced gaps.

The relative immunity of the proposed e-textile SWTL to cutting is demonstrated in Fig. 11. The 45 cm SWTL still maintained a relatively high S_{21} after cutting. For benchmarking, a microstrip line of 15 cm has been fabricated and measured before and after introducing a single cut in the centre of the signal trace. After cutting, the microstrip exhibited an S_{21} under -70 dB, demonstrating the advantage of using a surface-wave SWTL over a conventional Q-TEM textile-based transmission line. With up to three cuts through the SWTL, an S_{21} over -50 dB was still maintained through the SWTL from 1 to 4 GHz, demonstrating improved reliability and the ability to operate after mechanical damage.

On the other hand, the surface wave propagation is expected to be less immune to external coupling between closely-packed lines. This is attributed to the lower E-field confinement compared to a microstrip line or a CPW. A high mutual coupling between closely coupled lines will result in additional cross-talk between co-located transceivers, such cross-talk effects between co-located surface wave lines have not been investigated in previous works dealing with surface-wave transmission lines [1], [27], [30]. To demonstrate the SWTL's immunity to cross-talk, the lines shown in Fig. 5(a) and (b) were characterized as a four-port network to investigate the cross-talk between the adjacent lines. The four-port measurements were performed using the two-port VNA by terminating the unused ports with a 50 Ω SMA load, in the same position, and sequentially remeasuring the s-parameters over the unused ports. Fig. 12 shows the measured s-parameters of the coupled SWTLs, where it can be seen that the cross-talk level is consistently 10 dB lower than the transmitted signal.

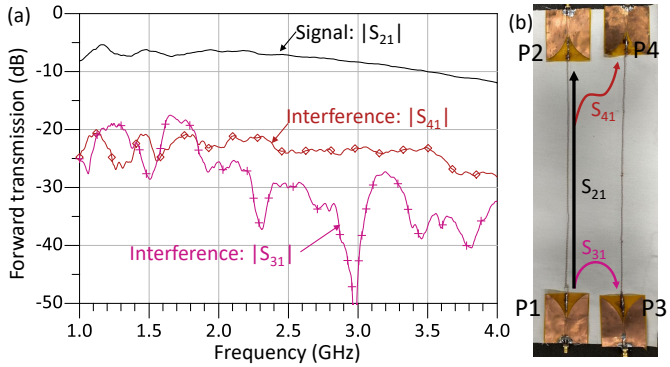

Fig. 12. (a) Measured four-port transmission properties of the closely-coupled SWTLs; (b) the port numbering and coupling mechanism.

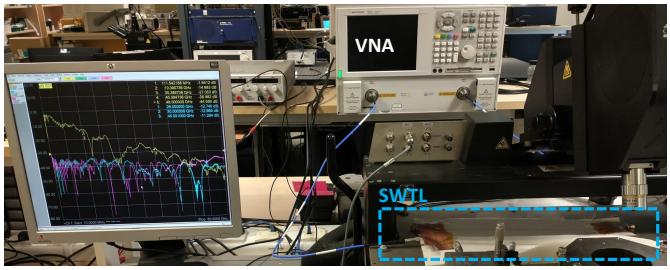

Fig. 13. The mmWave measurement setup of the shielded SWTL.

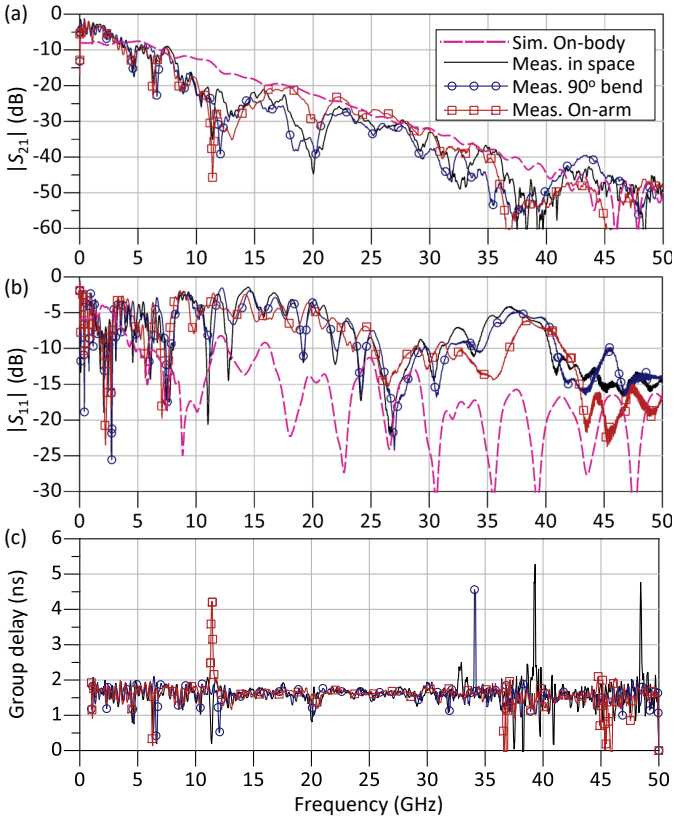

Fig. 14. Simulated and measured mmWave transmission properties of the SWTL: (a) forward transmission; (b) reflection coefficient; (c) group delay.

E. Low-Loss On-Body mmWave Transmission

The human body losses increase with frequency due to an increase in the tanδ losses [39]. This property makes on-body high-speed signaling, e.g. 5G/6G and 60 GHz point-to-point communication, a significant challenge due to the absorption by the human body. Nevertheless, recent work has shown the potential for comparable loss at 60 GHz to 900 MHz on-body links, when using aligned horn antennas placed on-body [21].

Surface wave propagation enables the on-body signal to overcome the path loss associated with spherical spreading as well as reduce the losses in the conductors and dielectrics forming the transmission line, compared to a standard TEM/Q-TEM line. The shielded SWTL was used for the mmWave on-body measurements to overcome the increased skin absorption beyond 20 GHz. The SMA connectors were replaced with 2.4 mm solder-terminated connectors to enable measurements up to 50 GHz. The s-parameters were measured using an Agilent E8361A PNA Network Analyzer, calibrated using a 1.85 mm SOLT E-calibration kit. The experimental setup for the mmWave measurements is shown in Fig. 13.

The 45 cm-long SWTL was experimentally characterized up to 50 GHz in three different cases. The first is the flat line shown in Fig. 13. The line was then measured with a 90° bend along its center, prohibiting a line-of-sight link between the transmitter a receiver. This use-case would prevent a directional on-body antenna such as a horn [21] or an end-fire Yagi-Uda [18] from maintaining high channel gain due to the main-lobe misalignment. The final measurement was performed on-body along the user's arm, as in Link 4 in Fig. 6. Fig. 14 shows the measured mmWave transmission properties of the SWTL up to 50 GHz. 1,001 frequency points were plotted, and the group delay was smoothed (i.e. moving averaged) by 0.1% to improve the graph's clarity.

Observing Fig. 14(a), it can be seen that the SWTL can support a relatively low-loss link on the human body up to 50 GHz (limited by the measurement setup). Furthermore, owing to the full shielding realized using a conductive fabric plane, the s-parameters of the SWTL experience minimal variations when positioned on-arm, i.e. L_4 from Fig. 6(a). Furthermore, both the simulated and measured $|S_{21}|$ are in good agreement. The phase stability of the S_{21} is demonstrated through the mostly uniform measured group delay, shown in Fig. 14(c). Apart from the observed spurious resonances, e.g. around 11 GHz for the on-arm case, the group delay exhibits under 0.5 ns ripple, which is remarkable for such a broadband on-body link operating up to 50 GHz. Owing to the difficulty in achieving a smooth transition between the 2.4 mm coaxial connectors and the CPW, attributed to the CPW's large width, the measured S_{11} exhibits a higher mismatch compared to its simulated counterparts, achieved using waveguide ports connected directly to the CPW. The measured ripple in the $|S_{21}|$ can also be attributed to the unstable $|S_{11}|$ response. However, based on the low attenuation over a long 45 cm link on-body, it can be concluded that the proposed e-textile SWTL is still a good candidate for low-loss broadband on-body up to mmWave frequencies. Compared to directional on-body radiative antennas, e.g. horns [21], the low-loss observed with a 90° bend demonstrates a significant advantage in enabling

TABLE I
COMPARISON WITH OTHER ON-BODY RF TRANSMISSION MECHANISMS.

	Transmission mechanism	**Attenuation α**	**Frequency**	**On-body loss***	**Launcher/ source size**	**Line dimensions**	**complexity**
This work	Shielded and Unshielded Textile Goubau SWTL	0.012 dB/mm at 1 GHz; 0.11 dB/mm at 50 GHz	0.5-4 GHz (unshielded); 0.5-50 GHz (shielded)	-4 to -17 dB at 45 cm (<4 GHz); -55 dB at 45 cm (50 GHz)	61×50 mm	40 μm diameter; conductive thread	very low, unpatterned wire over-stitched on any fabric
[1]	Textile spoof surface plasmon	NR	2.3-2.5 GHz	30–45 dB†	Similar width to lines	20-23 mm width	medium, specific line dimensions
[3]	Magneto-inductive planar NFC coils on textile	0.13–0.03 dB/mm at 13.56 MHz†	13.56 MHz	20 dB at 80 cm	180× 60 mm	6 cm wide	low, scalable coils fabricated using flexible metal
[40]	On-body flexible antennas	NA**	2 GHz	30 dB at 40 cm†	$\approx \lambda/4$	NA, radiative transmission	low, potential for textile antennas
[21]	On-body horn antennas	NA**	60 GHz	50–60 dB at 40 cm	WG25 waveguide + horn size	NA	high, non-textile horn antennas w/ alignment
[23]	Broadside PCB patches and on-body textile stripline	0.045 dB/mm at 2.4 GHz	2.4 GHz	23.3 LoS; 23.8 N-LoS	$\approx \lambda/2$ (patch dimensions)	6 mm width, 5–7 mm body clearance	medium, thick antenna/line with specific line dimensions
[10]	Magneto-inductive waveguide	0.01 dB/mm at 40 MHz†	40 and 80 MHz	under 10 dB†	NA	body-surrounding loops, diameter ≈10 cm ‡	low, unconnected loops
[22]	Conductive all-textile SIW	0.3 dB/mm at 35 GHz	33–37 GHz	NR, similar to away from body	Non-textile WR-28 port	3.85 mm wide	medium, destructive embroidery with waveguide transition
[6]	Printed silver textile microstrip	0.013 dB/mm at 1 GHz; 0.363 dB/mm at 50 GHz	(0.09–1.1) to 50 GHz	NR, similar to away from body	NA: no launcher	$1 < W < 10$ mm (substrate-dependent)	medium, screen-printable lines with controlled Z_0

NA: not applicable; NR: not reported; *insertion loss; **radiative transmission; † estimated from the graph; ‡estimated from the drawings/photographs.

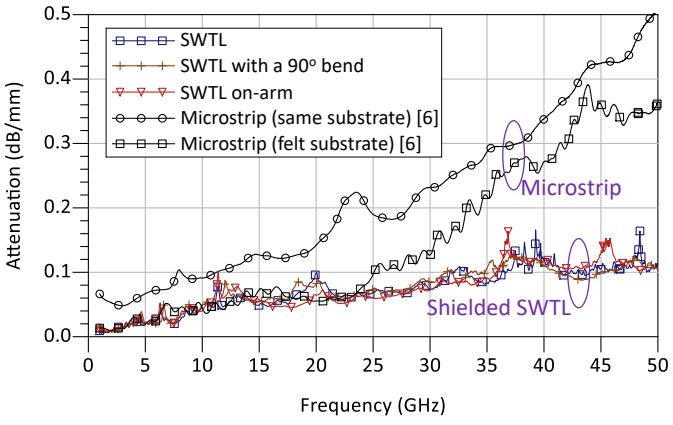

Fig. 15. Measured attenuation of the SWTL, normalized to the line's length, compared to the textile-based microstrip lines from [6]

non line-of-sight links.

The attenuation normalized to length of the SWTL has been normalized to its physical size to compare it to conventional on-body transmission lines. Fig. 15 shows the attenuation of the proposed SWTL compared to a printed textile-based microstrip line realized on the same substrate, as well as on a thicker felt fabric substrate. The losses of both microstrip lines are different due to being implemented of substrates of different heights, leading to lines of 1.7 and 6 mm width for the poly-cotton and felt substrates, respectively [6]. The difference in width results in different Ohmic resistances and subsequently attenuation, which becomes increasingly significant with the high surface roughness of textiles. Further details on the matching and design of the reference e-textile microstrip lines can be found in [6].

Observing the measured attenuation results in Fig. 15, it can be observed that both the SWTL and felt-based (low-resistance) microstrip line exhibit comparable attenuation below 20 GHz. Furthermore, owing to its shielding from the body, the SWTL losses do not increase in human proximity. Beyond 20 GHz, the microstrip lines exhibit increased attenuation due to the skin-depth effect and the high surface roughness of the fabric substrates [6]. Nevertheless, the losses in the SWTL exhibit minimal increase with frequency due to the EM propagation along the surface of the SWTL. At 50 GHz, the maximum attenuation incurred by the SWTL is 0.11 dB/mm, exhibiting its high suitability for on-body mmWave signaling.

To illustrate, with a microstrip line attenuation in excess of 0.35 dB/mm, a 450 mm-long link will incur an insertion loss over 150 dB, making it impossible to satisfy the link budget of a state-of-the-art mmWave communication system [41]. Therefore, the proposed SWTL not only represents a significantly simpler transmission line structure compared to a Z_0-controlled microstrip line but also incurs 80% lower losses compared to a microstrip line on the same substrate.

F. Comparison with State-of-the-Art

The proposed e-textile SWTL is compared to other on-body RF transmission mechanisms in Table I. The compared mechanisms include RF propagation using omnidirectional and directional antennas [21], [40], on-body waveguiding mechanisms such as magneto-inductive waveguides [3], [10], Spoof Surface Plasmon (SSP) metamaterials [1], all-textile SIW [22], and textile-based microstrip lines [6].

From the frequency of operation compared in Table I, it can be seen that the proposed shielded SWTL achieves an ultra-broadband operation range, only matched by a standard microstrip line [6]. Nevertheless, the SWTL maintains significantly lower attenuation compared to the textile-based microstrip, as previously shown in Fig. 15. While the low-frequency magneto-inductive waveguides, [3], [10], can achieve comparable attenuation to the proposed SWTL, they are restricted to applications under 80 MHz, limiting their suitability to low data-rate applications. In [21], aligned horns achieve a comparable path-loss on-body to the proposed SWTL over the same distance, such channel gain is however dependent on the horns' alignment and high gain. Therefore, the versatility of the proposed line, which can tolerate sharp bends and non-line-of-sight links, makes it a favorable option over high-gain on-body antennas.

In terms of complexity, the proposed SWTL is the least complex compared to other on-body waveguiding mechanisms. The proposed SWTL can be over-stitched onto pre-existing textiles for simpler integration into garments, making it similar to to laminated lines [6] and coils [3]. Moreover, the very small footprint of the single-thread line compared to SSP metamaterials, [1], makes it a more favorable choice for concealed textile-integrated RF transmission. In addition to the compared transmission mechanisms in Table I, textile waveguides based on electromagnetic bandgaps (EBGs) [42] exhibit higher attenuation than the proposed shielded SWTL, in addition to being significantly more complex and harder to assemble or manufacture. Therefore, the proposed shielded SWTL represents a feasible approach to low-loss low-complexity broadband on-body links up to mmWave bands.

IV. Conclusion

In this paper, the use of surface wave on-body links for low-loss ultra-broadband transmission up to 50 GHz was proposed based on a textile SWTL. It is demonstrated that SWTLs can be used to realize low-loss links in the UHF spectrum, exhibiting over 20 dB higher forward transmission compared to unconnected on-body antennas of larger dimensions. Using the proposed SWTL, non line-of-sight conformable links have been demonstrated over different body parts. At mmWave frequencies, the proposed shielded SWTL was demonstrated with an ultra-low attenuation of 0.11 dB/mm. The achieved mmWave transmission is unmatched by other existing technologies including textile-based microstrip lines, on-body directional antennas, as well as textile-based waveguides, and represents a four-fold improvement over a microstrip line implemented on the same substrate. Further advantages of the SWTL including improved immunity to cutting, low cross-talk, and low SAR have been demonstrated to show the SWTL's suitability for different on-body communication scenarios. It is concluded that SWTLs are highly suitable for low-loss broadband on-body transmission in future BANs, where the proposed SWTL could be applied to high data-rate transmission, simultaneous information and power transfer, and on-body non-invasive RF sensing.

Acknowledgment

The author would like to thank Harold Chong for providing the PNA E-calibration kit, and Abiodun Komolafe for his support with the lines fabrication.

Datasets used in this article are available from the University of Southampton repository at DOI: 10.5258/SOTON/D2072. Ethical approval has been obtained from the Faculty of Engineering and Physical Sciences (FEPS) Ethics Committee, University of Southampton, SO17 1BJ, application number: 64814, approved: 26/8/2021.

References

[1] X. Tian, P. M. Lee, Y. J. Tan, T. L. Y. Wu, H. Yao, M. Zhang, Z. Li, K. A. Ng, B. C. K. Tee, and J. S. Ho, "Wireless body sensor networks based on metamaterial textiles," *Nature Electronics*, vol. 2, pp. 243–251, 2019.

[2] J. Li, D. Y., J. Park, and J.Yoo, "Body-coupled power transmission and energy harvesting," *Nat Electron*, vol. 4, pp. 530–538, 2021.

[3] A. Hajiaghajani, A. H. A. Zargari, M. Dautta, A. Jimenez, F. Kurdahi, and P. Tseng, "Textile-integrated metamaterials for near-field multibody area networks," *Nat. Electron.*, 2021.

[4] A. Komolafe, B. Zaghari, R. Torah, A. S. Weddell, H. Khanbareh, Z. M. Tsikriteas, M. Vousden, M. Wagih, U. T. Jurado, J. Shi, S. Yong, S. Arumugam, Y. Li, K. Yang, G. Savelli, N. M. White, and S. Beeby, "E-textile technology review–from materials to application," *IEEE Access*, vol. 9, pp. 97 152–97 179, 2021.

[5] A. Kiourti, C. Lee, and J. L. Volakis, "Fabrication of Textile Antennas and Circuits With 0.1 mm Precision," *IEEE Antennas Wireless Propag. Lett.*, vol. 15, pp. 151 – 153, 2016.

[6] M. Wagih, A. Komolafe, and N. Hillier, "Screen-printable flexible textile-based ultra-broadband millimeter-wave dc-blocking transmission lines based on microstrip-embedded printed capacitors," *IEEE Journal of Microwaves*, vol. Unpublished, 2021.

[7] M. Wagih, G. S. Hilton, A. S. Weddell, and S. Beeby, "Broadband Millimetre-Wave Textile-based Flexible Rectenna for Wearable Energy Harvesting ," *IEEE Trans. Microw Theory Techn*, vol. 68 no. 11, pp. 4960 – 4972, 2020.

[8] N. Chahat, M. Zhadobov, S. A. Muhammad, L. L. Coq, and R. Sauleau, "60-GHz Textile Antenna Array for Body-Centric Communications," *IEEE Trans. Antennas Propag.*, vol. 61 no. 4, pp. 1816 – 1824, 2013.

[9] P. S. Hall and Y. Hao, "Antennas and propagation for body centric communications," in *2006 First European Conference on Antennas and Propagation*, 2006.

[10] V. Mishra and A. Kiourti, "Wearable planar magnetoinductive waveguide: A low-loss approach to wbans," *IEEE Transactions on Antennas and Propagation*, vol. 69, no. 11, pp. 7278–7289, 2021.

[11] A. Pellegrini, A. Brizzi, L. Zhang, K. Ali, Y. Hao, X. Wu, C. C. Constantinou, Y. Nechayev, P. S. Hall, N. Chahat, M. Zhadobov, and R. Sauleau, "Antennas and Propagation for Body-Centric Wireless Communications at Millimeter-Wave Frequencies: A Review [Wireless Corner]," *IEEE Antennas Propag. Magazine*, vol. 55 no. 4, pp. 262 – 287, 2013.

[12] M. Kim and J.-i. Takada, "Statistical model for 4.5-ghz narrowband on-body propagation channel with specific actions," *IEEE Antennas and Wireless Propagation Letters*, vol. 8, pp. 1250–1254, 2009.

[13] P. Hall, Y. Hao, and K. Ito, "Guest editorial for the special issue on antennas and propagation on body-centric wireless communications," *IEEE Transactions on Antennas and Propagation*, vol. 57, no. 4, pp. 834–836, 2009.

[14] A. Noda and H. Shinoda, "Inter-ic for wearables (i2we): Power and data transfer over double-sided conductive textile," *IEEE Transactions on Biomedical Circuits and Systems*, vol. 13, no. 1, pp. 80–90, 2019.

[15] C. Mendes and C. Peixeiro, "On-Body Transmission Performance of a Novel Dual-Mode Wearable Microstrip Antenna," *IEEE Trans. Antennas Propag.*, vol. 66 no. 9, pp. 4872 – 4877, 2018.

[16] N. Chahat, M. Zhadobov, L. L. Coq, and R. Sauleau, "Wearable Endfire Textile Antenna for On-Body Communications at 60 GHz," *IEEE Antennas Wireless Propag. Lett.*, vol. 11, pp. 799 – 802, 2012.

[17] A. Alemaryeen and S. Noghanian, "On-Body Low-Profile Textile Antenna With Artificial Magnetic Conductor," *IEEE Trans. Antennas Propag.*, vol. 67 no. 6, pp. 3649 – 3656, 2019.

[18] N. Chahat, M. Zhadobov, L. L. Coq, S. I. Alekseev, and R. Sauleau, "Characterization of the Interactions Between a 60-GHz Antenna and the Human Body in an Off-Body Scenario," *IEEE Trans. Antennas Propag.*, vol. 60 no. 12, pp. 5958 – 5965, 2012.

[19] J. Kimionis, A. Georgiadis, S. N. Daskalakis, and M. M. Tentzeris, "A printed millimetre-wave modulator and antenna array for backscatter communications at gigabit data rates," *Nat. Electron.*, 2021.

[20] Y. Wang, B. Liu, R. Wu, H. Liu, A. T. Narayanan, J. Pang, N. Li, T. Yoshioka, Y. Terashima, H. Zhang, D. Tang, M. Katsuragi, D. Lee, S. Choi, K. Okada, and A. Matsuzawa, "A 60-ghz 3.0-gb/s spectrum efficient bpook transceiver for low-power short-range wireless in 65-nm cmos," *IEEE Journal of Solid-State Circuits*, vol. 54, no. 5, pp. 1363–1374, 2019.

[21] R. Aminzadeh, A. Thielens, M. Zhadobov, L. Martens, and W. Joseph, "WBAN Channel Modeling for 900 MHz and 60 GHz Communications," *IEEE Trans. Antennas Propag.*, 2020 Early access, DOI: 10.1109/TAP.2020.3045498.

[22] L. Alonso-Gonzalez, S. Ver-Hoeye, C. Vazquez-Antuna, M. Fernandez-Garcia, and F. L.-H. Andres, "On the Techniques to Develop Millimeter-Wave Textile Integrated Waveguides Using Rigid Warp Threads," *IEEE Trans. Microw. Theory Techn.*, vol. 66, 2, pp. 751 – 761, 2018.

[23] T. T. Lan and H. Arai, "Propagation loss reduction between on-body antennas by using a conductive strip line," *IEEE Antennas and Wireless Propagation Letters*, vol. 17, no. 12, pp. 2449–2453, 2018.

[24] M. Wagih, A. S. Weddell, and S. Beeby, "Omnidirectional Dual-Polarized Low-Profile Textile Rectenna with over 50% Efficiency for Sub-μW/cm^2 Wearable Power Harvesting," *IEEE Transactions on Antennas and Propagation*, vol. 69, no. 5, pp. 2522–2536, 2021.

[25] N. Cho, J. Yoo, S.-J. Song, J. Lee, S. Jeon, and H.-J. Yoo, "The human body characteristics as a signal transmission medium for intrabody communication," *IEEE Transactions on Microwave Theory and Techniques*, vol. 55, no. 5, pp. 1080–1086, 2007.

[26] X. Tian, Q. Zeng, D. Nikolayev, and J. S. Ho, "Conformal propagation and near-omnidirectional radiation with surface plasmonic clothing," *IEEE Transactions on Antennas and Propagation*, vol. 68, no. 11, pp. 7309–7319, 2020.

[27] A. Sharma, A. T. Hoang, and M. S. Reynolds, "Long-range battery-free uhf rfid with a single wire transmission line," *IEEE Sensors Journal*, vol. 17, no. 17, pp. 5687–5693, 2017.

[28] T. Akalin, A. Treizebre, and B. Bocquet, "Single-wire transmission lines at terahertz frequencies," *IEEE Transactions on Microwave Theory and Techniques*, vol. 54, no. 6, pp. 2762–2767, 2006.

[29] J. Liang, C. Chiau, X. Chen, and C. Parini, "Study of a printed circular disc monopole antenna for uwb systems," *IEEE Trans. Antennas Propag.*, vol. 53, no. 11, pp. 3500 – 3504, 2005.

[30] A. Kianinejad, Z. N. Chen, and C.-W. Qiu, "Design and modeling of spoof surface plasmon modes-based microwave slow-wave transmission line," *IEEE Transactions on Microwave Theory and Techniques*, vol. 63, no. 6, pp. 1817–1825, 2015.

[31] A. Sharma, A. T. Hoang, and M. S. Reynolds, "A coplanar vivaldi-style launcher for goubau single-wire transmission lines," *IEEE Antennas and Wireless Propagation Letters*, vol. 16, pp. 2955–2958, 2017.

[32] M. Wagih, A. Komolafe, and B. Zaghari, "Dual-Receiver Wearable 6.78 MHz Resonant Inductive Wireless Power Transfer Glove Using Embroidered Textile Coils," *IEEE Access*, vol. 8, pp. 24 630 – 24 642, 2020.

[33] M. Wagih, G. S. Hilton, A. S. Weddell, and S. Beeby, "Dual-polarized wearable antenna/rectenna for full-duplex and mimo simultaneous wireless information and power transfer (swipt)," *IEEE Open Journal of Antennas and Propagation*, vol. 2, pp. 844–857, 2021.

[34] M. Wagih, Y. Wei, and S. Beeby, "Flexible 2.4 GHz Sensor Node for Body Area Networks with a Compact High-Gain Planar Antenna," *IEEE Antennas Wireless Propag. Lett.*, vol. 17, 12, pp. 49 – 53, 2018.

[35] M. Wagih, Y. Wei, A. Komolafe, R. Torah, and S. Beeby, "Reliable UHF Long-Range Textile-Integrated RFID Tag Based on a Compact Flexible Antenna Filament," *Sensors*, vol. 20 (12), p. 3435, 2020.

[36] S. A. Haydhah, F. Ferrero, L. Lizzi, M. S. Sharawi, and A. Zerguine, "A multifunctional compact pattern reconfigurable antenna with four radiation patterns for sub-ghz iot applications," *IEEE Open Journal of Antennas and Propagation*, vol. 2, pp. 613–622, 2021.

[37] R. Pei, M. P. Leach, E. G. Lim, Z. Wang, C. Song, J. Wang, W. Zhang, Z. Jiang, and Y. Huang, "Wearable ebg-backed belt antenna for smart on-body applications," *IEEE Transactions on Industrial Informatics*, vol. 16, no. 11, pp. 7177–7189, 2020.

[38] Z. Xu, T. Kaufmann, and C. Fumeaux, "Wearable textile shielded stripline for broadband operation," *IEEE Microwave and Wireless Components Letters*, vol. 24, no. 8, pp. 566–568, 2014.

[39] A. R. Guraliuc, M. Zhadobov, G. Valerio, N. Chahat, and R. Sauleau, "Effect of Textile on the Propagation Along the Body at 60 GHz," *IEEE Trans. Antennas Propag.*, vol. 62, 3, pp. 1489 – 1494, 2013.

[40] A. Thielens, R. Benarrouch, S. Wielandt, M. G. Anderson, A. Moin, A. Cathelin, and J. M. Rabaey, "A comparative study of on-body radio-frequency links in the 420 mhz–2.4 ghz range," *Sensors*, vol. 18, no. 12, 2018.

[41] C. W. Byeon, K. C. Eun, and C. S. Park, "A 2.65-pj/bit 12.5-gb/s 60-ghz ook cmos transmitter and receiver for proximity communications," *IEEE Transactions on Microwave Theory and Techniques*, vol. 68, no. 7, pp. 2902–2910, 2020.

[42] M. Elbacha, F. Ferrero, and L. Lizzi, "Wearable waveguide surface for low-loss body area network communications," *IEEE Antennas and Wireless Propagation Letters*, pp. 1–1, 2021.

Mahmoud Wagih (GS'18, M'21) received his B.Eng. (Hons.) in September 2018, and his Ph.D. on rectenna design in April 2021, both in Electrical and Electronic Engineering from the University of Southampton.

In 2017 he worked as a Research Assistant at the University of Southampton Malaysia. In 2018, he was a Hardware Engineering Intern at Arm, and, in 2020, a Research Intern at Arm, Cambridge, U.K. He is currently an RAEng UK IC Research Fellow at the University of Southampton, U.K. His interests broadly cover antennas and microwave systems for energy harvesting, sensing, and wearable applications. He has over 50 refereed journal and conference publications, and has delivered several invited webinars on these topics.

Dr. Wagih is a Senior Member of the International Union of Radio Science (URSI) and a member of the Institute of Engineering and Technology (MIET). He is an affiliate member of the IEEE Microwave Theory & Techniques Technical Committees TC-24 and TC-26. He was the recipient of the Best Undergraduate Project Prize, School Winner Doctoral Research Award, Best in Faculty Doctoral Research Award, and the Dean's Award for Early Career Researchers, in 2018-2021, at the University of Southampton. He was selected for the IEEE International Microwave Symposium Project Connect in 2019. He received the Best Student Paper Award at the IEEE Wireless Power Transfer Conference, 2019, the Best Oral Presentation at PowerMEMS, 2019, the Best Paper Award at PowerMEMS, 2021, was a Best Student Paper Finalist at IEEE WPTC, 2021, received the IEEE MTT-S Best 3MT Presentation Prize (second place) at the IEEE Microwave Week, 2020, and was a U.K. TechWorks Young Engineer of the Year finalist, in 2021. He was a session co-chair at EuCAP, 2021, and a TPC reviewer for various conferences including the IEEE International Microwave Symposium (IMS), and the IEEE Antennas and Propagation Symposium (APS). He acts as a reviewer for over eleven TRANSACTIONS and journals.